УДК 53.088:62 – 754.2 (045)

V. Apostolyuk

DEMODULATED KALMAN FILTERING FOR CORIOLIS VIBRATORY GYROSCOPES

Introduction

Many modern angular rate sensors operate using sensing of the Coriolis force induced motion in vibrating structures. Such approach allows to avoid using expensive means of mechanisation as well as to increase long term reliability of sensors. Another benefit lays in the possibility to fabricate sensitive elements of such gyroscopes in miniature form by using modern microelectronic mass-production technologies. Such gyroscopes are frequently referred to as MEMS (Micro-Electro-Mechanical-Systems) gyroscopes [1].

Being based on sensing of Coriolis acceleration due to the rotation in oscillating structures, CVGs have a lot more complicated mathematical models, comparing to the conventional types of gyroscopes. One of such complication is a result of the useful signal proportional to the external angular rate being modulated with the intentionally excited primary oscillations [2-4]. From the mathematical modeling point of view, this leads to necessity to "demodulate" the solution in terms of the sensitive element displacements to obtain practically feasible insights into CVG dynamics and errors. From the control systems point of view, conventional representation of CVGs incorporates primary oscillation excitation signal as an input to the dynamic system, and unknown angular rate as a coefficients of its transfer functions [4]. As a result, dynamics of CVGs has been analyzed mainly in steady state, while transient process analysis, for example, has been omitted due to its apparent complexity. Neither this allowed to synthesise efficient Kalman filters to improve performances of CVG.

This paper describes new state space models of demodulated CVG dynamics in terms of complex amplitude-phase variables, which enables having angular rate as a state vector component and allows synthesising linear Kalman filter to improve its performances.

Problem Formulation

In order to solve the problem of linear Kalman filtering of CVG, we have to produce state space models of its dynamics, where angular rate it included into the state vector, rather than being parameter of the model. Performance of the

obtained linear Kalman filter should be verified using realistic numerical simulations.

CVG Dynamics in State Space Representation

Sensitive element of the most CVGs can be represented as a massive element (proof mass m_2 in Fig. 1) attached to the basis by means of set of springs and the decoupling frame m_1.

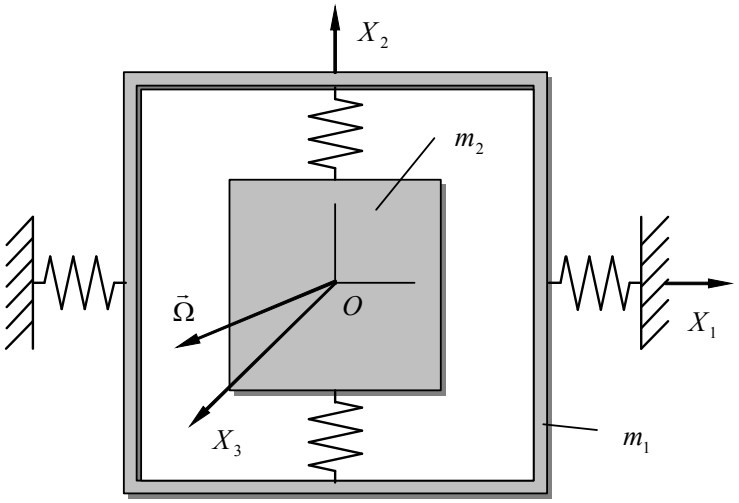

Fig. 1. CVG sensitive element

Here springs may allow either translational or rotational motion of the proof mass and decoupling frame. Primary oscillations of the sensitive element are excited along the axis X_1, and secondary oscillations of the proof mass due to the angular rate $\vec{\Omega}$ are detected along the axis X_2.

In the most generalized form, motion equations of the CVG sensitive element both with translational and rotational motion could be represented in the following form [4]:

$$\begin{cases} \ddot{x}_1 + 2\zeta_1 k_1 \dot{x}_1 + (k_1^2 - d_1\Omega^2)x_1 + g_1\Omega\dot{x}_2 + d_3\dot{\Omega}x_2 = q_1(t), \\ \ddot{x}_2 + 2\zeta_2 k_2 \dot{x}_2 + (k_2^2 - d_2\Omega^2)x_2 - g_2\Omega\dot{x}_1 - \dot{\Omega}x_1 = q_2(t). \end{cases} \quad (1)$$

Here x_1 and x_2 are the generalized coordinates that describe primary (excited) and secondary (sensed) motions of the sensitive element respectively, k_1 and k_2 are the corresponding natural frequencies, ζ_1 and ζ_2 are the dimensionless relative damping coefficients, Ω is the measured angular rate, which is orthogonal to the axes of primary and secondary motions, q_1 and q_2 are the generalized accelerations due to the external forces acting on the sensitive element. The remaining dimensionless coefficients are different for the sensitive elements exploiting either translational or rotational motion. For the translational sensitive element they are $d_1 = d_2 = 1$, $d_3 = m_2/(m_1 + m_2)$, $g_1 = 2m_2/(m_1 + m_2)$,

$g_2 = 2$, where were m_1 and m_2 are the masses of the outer frame and the internal massive element. In case of the rotational motion of the sensitive element, these coefficients are the functions of different moments of inertia (for greater details see [4]).

The most straightforward transition from the equations (1) to the state space representation is implemented as follows:

$$\begin{cases} \dot{X} = A \cdot X + B \cdot U, \\ Y = C \cdot X. \end{cases} \tag{2}$$

Here newly introduced vectors and matrices have the following meaning:

$$X = \{x_1 \quad \dot{x}_1 \quad x_2 \quad \dot{x}_2\}',$$
$$U = \{0 \quad q_1 \quad 0 \quad q_2\}^T,$$
$$A = \begin{bmatrix} 0 & 1 & 0 & 0 \\ -k_1^2 + d_1\Omega^2 & -2\zeta_1 k_1 & -d_3\dot{\Omega} & -g_1\Omega \\ 0 & 0 & 0 & 1 \\ \dot{\Omega} & g_2\Omega & -k_2^2 + d_2\Omega^2 & -2\zeta_2 k_2 \end{bmatrix}, \tag{3}$$
$$B = \begin{bmatrix} 0 & 0 & 0 & 0 \\ 0 & 1 & 0 & 0 \\ 0 & 0 & 0 & 0 \\ 0 & 0 & 0 & 1 \end{bmatrix}, \; C = \begin{bmatrix} 1 & 0 & 0 & 0 \\ 0 & 0 & 1 & 0 \end{bmatrix},$$

where superscript in $\{...\}'$ hereafter means vector transposing. Analysing (3) one should note, that in the state space representation (2) matrix A depends on the yet unknown angular rate Ω. Expanding state vector X to include angular rate as a state variable will make system (2) non-linear, which is highly undesirable. Moreover, observed state includes position of the sensitive element that in vibratory gyroscopes varies with high frequencies. This means, that Kalman filtering must work with small time latencies, which significantly increases the requirements for the computational hardware. In order to avoid these problems, let us use demodulated dynamics of CVGs ([5]) to produce feasible designs of the Kalman filters.

Assuming settled primary oscillations, motion equations (1) can be transformed to the following demodulated amplitude-phase form [5]

$$\ddot{A}_2 + 2(\zeta_2 k_2 + j\omega)\dot{A}_2 + (k_2^2 - \omega^2 + 2j\omega k_2\zeta_2)A_2 = (j\omega g_2\Omega + \dot{\Omega})A_1. \tag{4}$$

Here $A_2(t) = A_{20}(t)e^{j\varphi_{20}(t)}$ is the complex amplitude of the secondary oscillations, in which A_{20} is the amplitude of the secondary oscillations and φ_{20} is its phase. Corresponding complex amplitude of the settled primary oscillations is

$$A_1 = \frac{q_{10}}{k_1^2 - \omega^2 + 2jk_1\zeta_1\omega}, \tag{5}$$

where ω is the excitation frequency and q_{10} is the amplitude of the primary excitation.

Let us now represent equation (4) in a standard state space form, where observed inputs are absent, but the angular rate is included in the state vector:

$$\begin{cases} \dot{X} = A \cdot X, \\ Y = C \cdot X. \end{cases} \tag{6}$$

Here newly introduced vectors and matrices have the following meaning:

$$X = \{A_2 \quad \dot{A}_2 \quad \Omega \quad \dot{\Omega}\}',$$

$$A = \begin{bmatrix} 0 & 1 & 0 & 0 \\ -k_2^2 + \omega^2 - 2j\omega k_2\zeta_2 & -2(\zeta_2 k_2 + j\omega) & j\omega g_2 A_1 & A_1 \\ 0 & 0 & 0 & 1 \\ 0 & 0 & 0 & 0 \end{bmatrix}, \tag{7}$$

$$C = \begin{bmatrix} 1 & 0 & 0 & 0 \end{bmatrix}.$$

One should note, that although angular rate is included in the state vector, system remains linear. Here we also assumed that angular acceleration is negligibly small, which is reflected by the zeroed last row of the matrix A in (7). However, both system matrix A and state vector X are complex valued, which may complicate its implementation using third party software.

Following the suggested in [5] procedure and neglecting higher order derivatives of the complex secondary amplitude ($\ddot{A}_2 \approx 0$), we can obtain the following slow motion equation:

$$2(\zeta_2 k_2 + j\omega)\dot{A}_2 + (k_2^2 - \omega^2 + 2j\omega k_2\zeta_2)A_2 = (j\omega g_2\Omega + \dot{\Omega})A_1. \tag{8}$$

In this case state-space equation (6) will have reduced order state vector and corresponding matrices:

$$X = \{A_2 \quad \Omega \quad \dot{\Omega}\}',$$

$$A = \frac{1}{2(\zeta_2 k_2 + j\omega)} \begin{bmatrix} -k_2^2 + \omega^2 - 2j\omega k_2\zeta_2 & j\omega g_2 A_1 & A_1 \\ 0 & 0 & 2(\zeta_2 k_2 + j\omega) \\ 0 & 0 & 0 \end{bmatrix}, \tag{9}$$

$$C = \begin{bmatrix} 1 & 0 & 0 \end{bmatrix}.$$

Again, angular accelerations are neglected and state vector is complex valued. This last complication can be overcome by assuming equal primary and secondary natural frequencies ($k_1 = k_2 = k$), equal damping ratios ($\zeta_1 = \zeta_2 = \zeta$), primary resonance excitation ($\omega = k\sqrt{1 - 2\zeta^2}$), and constant angular rate ($\dot{\Omega} \approx 0$). As a result, we can obtain simplified differential equation for the real secondary amplitude A_{20}:

$$\dot{A}_{20} = -k\zeta A_{20} + \frac{g_2 q_{10}\sqrt{1-2\zeta^2}}{4\zeta k^2(1-\zeta^2)}\Omega. \tag{10}$$

This leads us to the simplest so far state space representation for CVGs:

$$X = \{A_{20} \quad \Omega\}',$$
$$A = \begin{bmatrix} -k\zeta & \frac{g_2 q_{10}\sqrt{1-2\zeta^2}}{4\zeta k^2(1-\zeta^2)} \\ 0 & 0 \end{bmatrix}, \; C = \begin{bmatrix} 1 & 0 \end{bmatrix}. \tag{11}$$

At this point we have real valued state vector and matrices in (11). The latest improvement to the system representation can be made by taking into account the fact that the output of the actual gyro is the measured angular rate, rather than amplitude of the secondary oscillations. In this case equation (10) can be rewritten as

$$\dot{\Omega}_* = -k\zeta\Omega_* + k\zeta\Omega, \tag{12}$$

where Ω_* is the measured angular rate at the gyro output, which in steady state becomes equal to the actual angular rate Ω. State vector and system matrices (11) become:

$$X = \{\Omega_* \quad \Omega\}',$$
$$A = \begin{bmatrix} -k\zeta & k\zeta \\ 0 & 0 \end{bmatrix}, \; C = \begin{bmatrix} 1 & 0 \end{bmatrix}. \tag{13}$$

Simplified mathematical model comprised of the equations (10) and (12) and the expressions (11) and (13) has been derived using many seemingly farfetched assumptions. Parameters of real gyroscopes most likely will be somewhat different from the assumed one. From this point of view, accuracy of the simplified model must be verified against variations of the actual CVG sensitive element parameters, such as natural frequencies and relative damping coefficients. As a model performance criterion let us choose the following integral:

$$J(\delta k, \delta\zeta) = \int_0^T [A_{20}(t) - A_{20}^*(t)]^2 dt. \tag{14}$$

Here $\delta k = k_2 / k_1$ is the ratio of the natural frequencies, $\delta\zeta = \zeta_2 / \zeta_1$ is the ratio of the relative damping ratios, $A_{20}^*(t)$ is the demodulated secondary amplitude produced by the "realistic" model (1). Graphic plot of the functional (14) is shown below in Fig. 2.

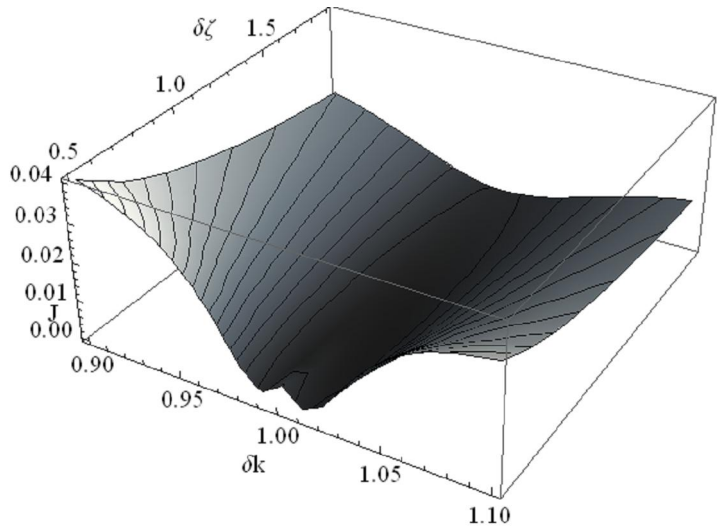

Fig. 2. Integral error of the simplified model

In this figure lower darker area in the middle corresponds to the highest accuracy of the simplified model for the perfectly matched sensitive element. Another useful feature of the simplified model is its insensitivity to the relative damping variations, which is often the case in real gyroscopes.

Kalman Filter Synthesis

The reason to use Kalman filter for CVGs is to be able to estimate secondary amplitude with greater accuracy by removing effects from process noise (disturbances) and measurement noise. In order to implement Kalman filter we have to derive difference model of the CVG dynamics in the following form:

$$\begin{cases} X_n = F \cdot X_{n-1} + w_{n-1}, \\ Z_n = H \cdot X_n + v_n. \end{cases} \quad (15)$$

Here X_n is the sampled state vector, Z_n is the measured state vector, $H = C$ is the state measurement matrix, w_n and v_n are the process and sensor noises respectively, and F is the state transition matrix, which can be calculated from the system matrix A using inverse Laplace transformation L^{-1} [6]

$$F = L^{-1}\{(I \cdot s - A)^{-1}\}, \quad (16)$$

where I is the identity matrix of the same size with A and s is the Laplace variable. This approach to calculation of transition matrix is practical since close-form solution of the equation (10) or (12) can be easily obtained due to its simplicity. Close-form solutions of other demodulated models also can be obtained, but they are cumbersome enough not to be presented in this paper.

Applying formula (16) to the matrix A from (13) results in the transition matrix for the simplified CVG model:

$$F = \begin{bmatrix} e^{-k\zeta t} & 1-e^{-k\zeta t} \\ 0 & 1 \end{bmatrix}. \tag{17}$$

Having calculated state transition matrix (17) we can now verify state observability for the simplified model as follows [6]:

$$Q_O = \begin{bmatrix} H \\ H \cdot F \end{bmatrix} = \begin{bmatrix} 1 & 0 \\ e^{-k\zeta t} & 1-e^{-k\zeta t} \end{bmatrix}. \tag{18}$$

Observability matrix Q_O given by (18) has full rank equal to 2, which satisfy condition for the state observability.

Governing equations for the discrete Kalman filter are as follows. Estimation of the system state X_n^- and error covariance matrix P_n^- are predicted as

$$\begin{aligned} X_n^- &= F \cdot \hat{X}_{n-1}, \\ P_n^- &= F \cdot \hat{P}_{n-1} \cdot F' + Q, \end{aligned} \tag{19}$$

where Q is the process noise w_n covariance. Next we calculate Kalman gain K_n and corrected estimations of the system state $\hat{X}_n$ and error covariance matrix $\hat{P}_n$ using the following expressions:

$$\begin{aligned} K_n &= P_n^- \cdot H' \cdot (H \cdot P_n^- \cdot H' + R)^{-1}, \\ \hat{X}_n &= X_n^- + K_n \cdot (Z_n - H \cdot X_n^-), \\ \hat{P}_n &= (I - K_n \cdot H) \cdot P_n^-. \end{aligned} \tag{20}$$

Here R is the sensor noise v_n covariance. Calculated by (20) estimations of the system state and error covariance matrix are then used in (19) to make their next step prediction.

Realistic CVG Simulation

In order to simulate Kalman filter operation and verify its efficiency it is reasonable to apply it to the realistically modelled gyro, rather than to the numerically simulated using simplified model like (12), for example. For this let us use numerical model given by equations (1). Its implementation in Simulink/Matlab software is shown in Fig. 3.

Kalman filter block from the Signal Processing Blockset is attached to the already demodulated output rate. Demodulation is performed by means of multiplying secondary oscillations with the synchronous sine signal and then filtering using low-pass filter, as shown in Fig. 3. Angular rate has shape of squared pulses with 1 rad/s amplitude. White noise is added to the output rate prior to be fed to the Kalman filter block.

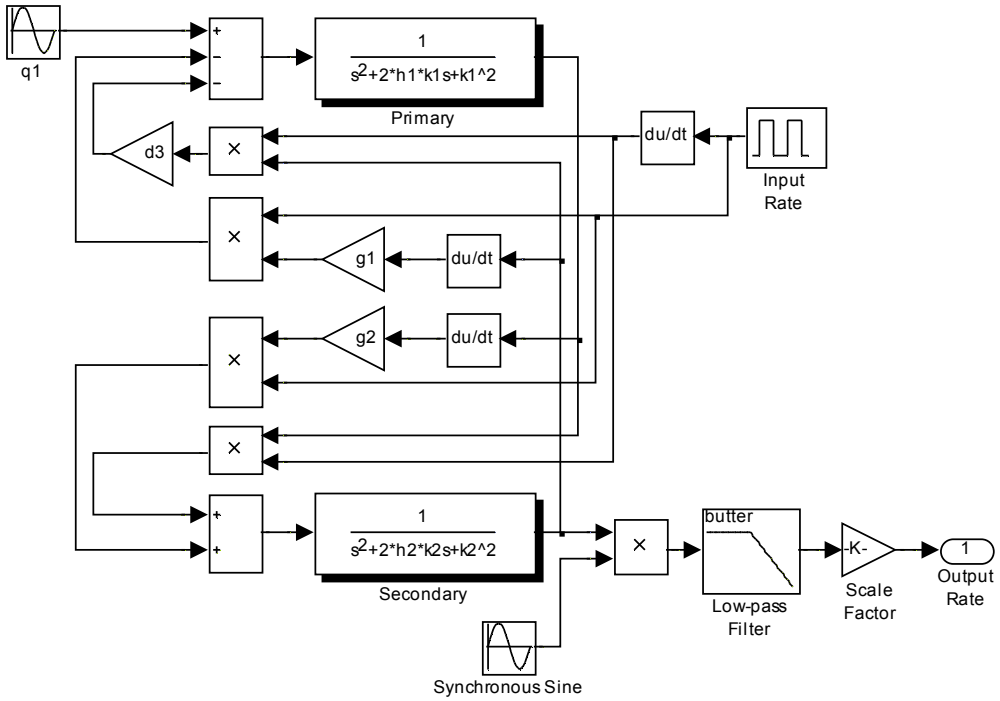

Fig. 3. Realistic model of CVG dynamics with synchronous demodulation

Filtering with Angular Random Walk

Let us now study performance of the Kalman filter applied to the realistically modelled CVG and synthesised using simple model (12). In this model input angular rate is assumed to be constant, while in reality it is not. To allow some variations in the input angular rate estimations, let us represent it by means of the random walk model. In order to this, we simply assume presence of a weak white noise as a process noise for the second component of the state vector, which is input angular rate that we want to estimate. Results of the numerical simulations are shown in Fig. 4 and 5.

The following parameters of the CVG were used in simulations: $k = 500Hz$, $\zeta = 0.025$. Zero initial conditions were chosen for the state vector and identity matrix has been used as an initial for the error covariance. Other parameters of the filter are as follows:

$$Q = \begin{bmatrix} 0 & 0 \\ 0 & 2 \cdot 10^{-6} \end{bmatrix}, \; R = 0.01.$$

Analyzing graphs in Fig. 4 and 5 one should see, that added sensor noise has been successfully removed from the output, while input angular rate has been estimated with some errors, however closer to the actual square pulse shape than measured output.

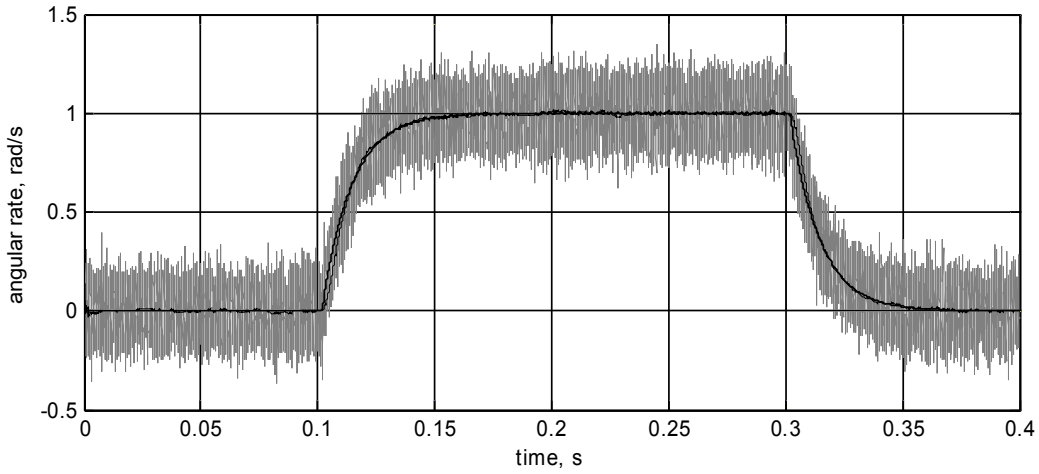

Fig. 4. Angular rate measurements
(gray – noised output, dotted – actual output without noise, solid – output estimation)

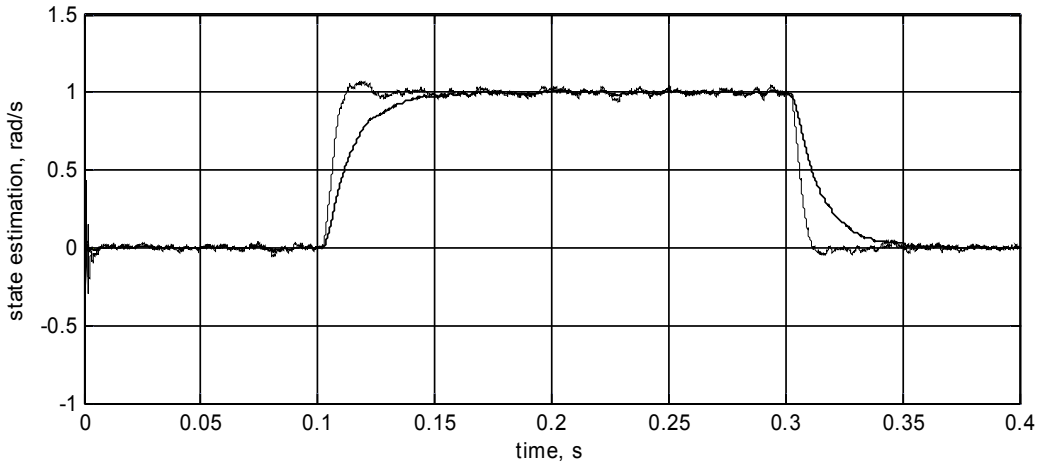

Fig. 5. State estimations over time
(solid – input angular rate, dashed – output angular rate)

Comparing sensor noise filtering using linear Kalman filter with the filtering by means of optimal static Wiener filter [7] demonstrates slight advantage of the Kalman filter approach.

Filtering with Low-Pass Angular Rate

Let us now consider the case, that angular rate is produced by the moving vehicle. In this case it can be modelled by means of a low-pass system described by the following equation:

$$\dot{\Omega} = -B \cdot \Omega + B \cdot \delta, \tag{21}$$

where B is the vehicle bandwidth, δ is the white noise. System matrix (13) and corresponding transition matrix (17) now become

$$A = \begin{bmatrix} -k\zeta & k\zeta \\ 0 & -B \end{bmatrix},$$
$$F = \begin{bmatrix} e^{-k\zeta t} & \dfrac{e^{-k\zeta t} - e^{-Bt}}{B - k\zeta} k\zeta \\ 0 & e^{-Bt} \end{bmatrix}. \tag{22}$$

One should note, that if $B = 0$ then matrices A and F become the ones from the previous model.

Simulation results for the state estimations of the low-pass angular rate case are shown in Fig. 6.

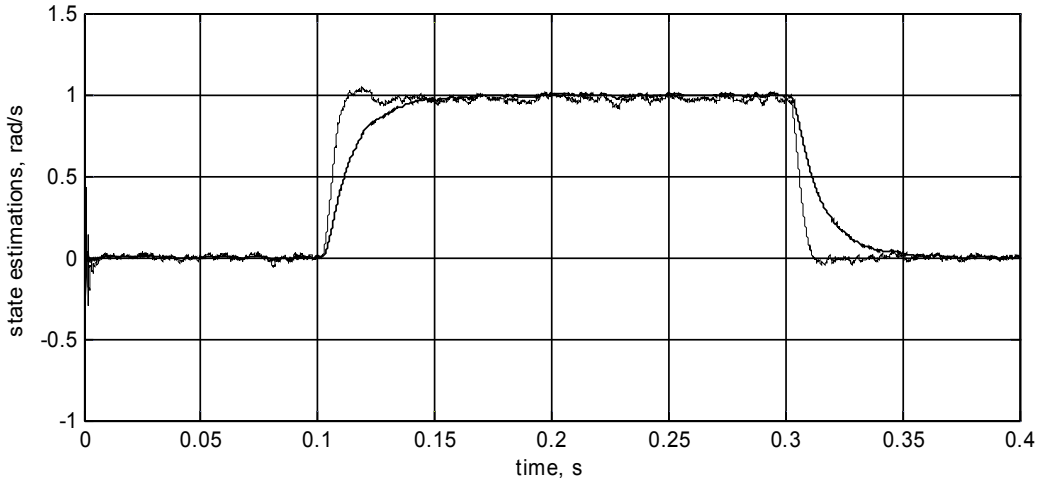

Fig. 6. State estimations over time
(solid – input angular rate, dashed – output angular rate)

Process and sensor noise covariance matrices were taken the same with the previous case, and bandwidth has been chosen $B = 1Hz$.

From the graph in Fig. 6 one can see that introducing bandwidth of the angular rate does not deliver any essential improvements to the quality of the input estimation. Moreover, as extensive analysis has demonstrated, increasing bandwidth introduces steady state errors to the input angular rate estimation.

Conclusions

Presented above analysis of the demodulated dynamics of CVG allowed to produce simple and yet accurate models with respect to the angular rate as an input. These models were successfully utilised to synthesise digital Kalman filters capable of efficiently removing sensor noise. Comparison of two cases, where input angular rate has been represented by means of a random walk and a low

pass random walk, demonstrated sufficient efficiency of the random walk model and absence of necessity to use more elaborated approaches. Estimating angular rate as a state vector component made possible to improve bandwidth of CVG at a cost of lesser noise cancellation.

Incorporating obtained model to synthesise Kalman filters targeted at identification of CVG parameters is viewed as an obvious continuation of the presented above research.

Acknowledgments

Here I would like to express my deep and sincere gratitude to Ms. Veronika Kotlyarevska, who sacrificed a lot to make this research possible.

References

1. *Yazdi N.* Micromachined Intertial Sensors / N. Yazdi, F. Ayazi, K. Najafi // Proceedings of the IEEE. – 1998. – Vol. 86, No. 8. – P. 1640-1659.
2. *Friedland B.* Theory and error analysis of vibrating-member gyroscope / B. Friedland, M.F. Hutton // IEEE Transactions on Automatic Control. – 1978. – no. 23. – P. 545-556.
3. *Lynch D.* Vibratory gyro analysis by the method of averaging / D. Lynch // Proc. 2nd St. Petersburg Conf. on Gyroscopic Technology and Navigation, St. Petersburg. – 1995. – P. 26-34.
4. *Apostolyuk V. A.* Theory and Design of Micromechanical Vibratory Gyroscopes / V. A. Apostolyuk // MEMS/NEMS Handbook (Ed: Cornelius T. Leondes), Springer. – 2006. – Vol.1, Chapter 6. – P. 173-195.
5. *Apostolyuk V.A.* Dynamics of Coriolis Vibratory Gyroscopes in Control Systems / V.A. Apostolyuk // Systems of Control, Navigation, and Communication. – 2010. – No. 1 (13) . – P. 62-66.
6. *Bar Shalom Y.* Estimation with Applications to Tracking and Navigation / Y. Bar Shalom, X. Rong Li, Thiagalingam Kirubarajan // Wiley & Sons. – 2001. – 558 p.
7. *Apostolyuk V.* Optimal Sensor Noise Filtering for Coriolis Vibratory Gyroscopes / V. Apostolyuk // Механіка гіроскопічних систем.– 2010.– №22.– С.5-12.